Journal of the Korean Society of Manufacturing Technology Engineers 27:2 (2018) 83~91

https://doi.org/10.7735/ksmte.2018.27.2.83

J. Korean Soc. Manuf. Technol. Eng.
ISSN 2508-5107(Online) / ISSN 2508-5093(Print)

Best Paper of This Month

State Observer-Based Backstepping Terminal Sliding Mode Control for Rectangular Robot Systems

Inseok-Seo[a], Hyunjae-Ryu[b], Seongik-Han[c*]

[a] School of Mechanical Engineering, Pusan National University,
2, Busandaehak-ro 63beon-gil, Geumjeong-gu, Busan 46241, Korea
[b] Pusan Robot Industry Association,
2, Busandaehak-ro 63beon-gil, Geumjeong-gu, Busan 46241, Korea
[c] Department of Mechanical System Engineering, Dongguk University Geongju Campus,
123, Dongdae-ro, Gyeongju, Gyeongbuk-do, 38066, Korea

ARTICLE INFO

Article history:
Received 15 December 2017
Revised 6 February 2018
Accepted 12 February 2018

Keywords:
Rectangular robot system
Super-twisting state observer
Backstepping control
Terminal sliding mode control

ABSTRACT

This study focuses on the fast state estimation of unmeasured state variable and uncertainty by using super-twisting state observer and adaptive law, and the design of a backstepping-based terminal sliding mode controller for rectangular robot systems. Introducing a super-twisting state observer can estimate unmeasured velocity information more rapidly than a conventional high-gain state observer. A backstepping controller with super-twisting observer is combined with a terminal sliding mode control scheme, which demonstrates faster error convergence performance than conventional backstepping sliding mode control. This estimation law, combined with the robustness of the controller for unknown states and dynamics, results in outstanding control performance when compared to conventional model-based computed torque control methods. The stability of the proposed control system was verified by using the Lyapunov-candidate-function. Comparative simulation and experimental results for the two-axis rectangular robot system demonstrate the efficacy of the proposed control scheme.

1. Introduction

In the industrial manufacturing fields, mechanical servo systems such as machine tool, rectangular robot manipulator, and automation devices, etc., have been taken as essential components. Thus, an exact operating motion of servo systems like rectangular robot system has been considered as important issue for manufacturing high quality several products. However, in the rectangular robot systems, there have been many problems such as dynamic parameter identification, nonlinearities of friction and deadzone, measurement problem of unmeasured variables. In the industrial field, PI and PID controller have been traditionally used to compensate the uncertainties. However, the gain tuning for optimized gain is bored and repeated large time-consuming work. It cannot guarantee rigorously the robustness the uncertainty. As an important problem in the rectangular robot systems, the velocity information is not directly measured because the linear scale or rotary encoder sensors is generally equipped in the linear motion system or motor system. By differentiating the position signal obtained from the linear scale or rotary encoder, the velocity information is obtained. Thus, because the noisy

* Corresponding author. Tel.: +82-54-770-2222
Fax: +82-54-770-2870
E-mail address: skhan@dongguk.ac.kr (Seongik Han).

signal is included in the obtained velocity, if the low-pass filter to remove noisy signal, the velocity information is distorted. As the frequently used state observer, the high-gain observer was developed[1-4]. To improve the performance of the state observer, the super-twisting sliding observer as a sort of the second order sliding mode observer was recently developed[5].

On the other hand, backstepping control[6] was developed to control complex nonlinear system by recursive procedure without using linearization. This control can be applied to general system and can be combined with other control method such as fuzzy[7] and neural networks[8]. Sliding mode control was also combined with backstepping control to enforce robustness to uncertainty[9]. Terminal sliding mode control[10] was developed to obtain faster convergence time than the normal sliding mode control. However, until now, backstepping control with terminal sliding mode was not developed and moreover super-twisting observer was not also combined into this backstepping based sliding mode controller. Therefore, the proposed control has more improved estimation performance and fast tracking error convergence than the conventional high-gain observer and sliding mode based control systems. In addition, the unknown dynamic parameters such as inertia, coupled centripetal Coriolis term, gravity, and deadzone width, are selected as assumed diagonal gain to fasten controller design time. These assumed parameters are used as feedforward compensator. Finally, the 2-axis rectangular robot system is selected to verify the performance of the proposed control scheme. Simulation and experimental results are presented to support the reasonability of the proposed control scheme.

2. Problem Formulation

The general model of the rectangular robot is described as follows:

$$M(q)\ddot{q} + C(q,\dot{q})\dot{q} + G(q) + F_f + F_d(t) = D(v(t)) \tag{1}$$

where $q, \dot{q}, \ddot{q} \in R^n$ are generalized position, velocity, and acceleration, respectively; $M(q) \in R^{n\times n}$ denotes the positive definite inertia matrix; $C(q,\dot{q}) \in R^{n\times n}$ denotes the centripetal Coriolis matrix; $G(q) \in R^{n\times 1}$ denotes the gravitational vector; $F_f(t) \in R^{n\times 1}$ denotes the friction vector, $F_d(t) \in R^{n\times 1}$ denotes the disturbance vector; and $u \in R^{n\times 1}$ is the control input vector.

Property 1. $M(q)$ and $G(q)$ are uniformly bounded and continuous for an uniformly bounded and continuous generalized position vector q.

Property 2. $C(q,\dot{q})$ is uniformly bounded and continuous for an uniformly bounded and continuous generalized position and velocity vectors q and $\dot{q}$.

Property 3. $\dot{q}^T[\dot{M}(q) - 2C(q,\dot{q})]\dot{q} = 0$ holds from the skew-symmetric property between $\dot{M}(q)$ and $C(q,\dot{q})$.

Assumption 1. $M(q)$, $C(q,\dot{q})$, $F_f(t)$, and $F_d(t)$ are bounded such that $\|M(q)\| \le \rho_M$, $\|C(q,\dot{q})\| \le \rho_c$, $\|F_f\| \le \rho_f$, and $\sup_{t\ge 0}\|F_d(t)\| \le \rho_d$, in which ρ_i are unknown positive finite constant vectors.

The deadzone function is defined as

$$w(t) = D(v(t)) = \begin{cases} m_l(v(t) + b_l), & v(t) \le -b_l \\ 0, & b_l < v(t) < b_r \\ m_r(v(t) - b_r), & v(t) \le b_r \end{cases}. \tag{2}$$

The deadzone width $b_l, b_r \ge 0$ are assumed as equal and unknown. m_l and m_r represent the deadzone slope functions and is assumed to have unit values. The concept of compensating deadzone effect[11,13] is to use inverse function $v(t) = D^{-1}(w(t))$ such that $D(D^{-1}(w(t)) = v(t)$ from the controller to achieve control without deadzone can be obtained as

$$v(t) = \begin{cases} w_d - \hat{b}_l, & w_d \le 0 \\ w_d + \hat{b}_r, & w_d > 0 \end{cases}. \tag{3}$$

therefore, $\hat{b}_r$ and $\hat{b}_l$ denote the estimated value of b_r and b_l, respectively. The unknown lumped deadzone parameter $\Delta D(v) = w - w_d = \Delta D_r p + \Delta D_l(1-p)$ is bounded such that $\|\Delta D\| \le \rho_d$, and $p = 1$ if $u \ge 0$, $p = 0$ if $u < 0$ and unknown deadzone parameters ΔD_r and ΔD_l are also bo unded.

Remark 1. The deadzone width in (4) is estimated by iterative trial and error method because experimental identification is cumbersome and time-consuming work.

$$\begin{aligned} \dot{x}_1 &= x_2 \\ \dot{x}_2 &= -M^{-1}(Cx_2 + G) - M^{-1}(F_f + F_d - \Delta D(u)) + M^{-1}w \\ y(t) &= x_1 \end{aligned} \tag{4}$$

where $x_1 = q$ and $x_2 = \dot{q}$.

Assumption 2. There are positive constants, δ_M, δ_C, and δ_G

that satisfy the following conditions:

$$\begin{cases} \|\Lambda_M - M(q)\| \le \delta_M \\ \|\Lambda_C - C(q,\dot{q})\| \le \delta_C \\ \|\Lambda_G - G(q)\| \le \delta_G \end{cases}, \tag{5}$$

in which $\Lambda_M \in R^{n\times n}$ and $\Lambda_C \in R^{n\times n}$ are positive finite diagonal matrices, and $\Lambda_G \in R^{n\times 1}$ is a positive finite constant vector.

Remark 2. The design gain parameters, $\Lambda_M \in R^{n\times n}$, $\Lambda_C \in R^{n\times n}$, and $\Lambda_G \in R^{n\times 1}$ are selected through an iterative trial and error assumption method without using complex identification process or approximation of fuzzy and neural networks.

The state space model of (5) can be approximately written as follows:

$$\begin{aligned} \dot{x}_1 &= x_2 \\ \dot{x}_2 &= -\Lambda_M^{-1}(\Lambda_C x_2 + \Lambda_G) + d(x,t) + \Lambda_M^{-1} w_d \\ y(t) &= x_1 \end{aligned} \tag{6}$$

where $x_1 = q$, $x_2 = \dot{q}$, $d(x,t) = -M^{-1}(F_f + F_d) + \Delta D + \delta_T$ and δ_T is the lumped total approximation error.

3. Design of Controller and Observer of the State and Disturbance

3.1 Design of Super-Twisting State Observer

In (5), although the state variables in (1) are available, however, the state variables x_2 is not measurable directly. Therefore, we introduce the super-twisting state observer[5,13]. A modified super-twisting state observers, in which contains a disturbance estimate, are designed as

$$\begin{aligned} \dot{\hat{x}}_1 &= \hat{x}_2 + \zeta_1 |\tilde{x}_1|^{1/2} sign(\tilde{x}_1), \\ \dot{\hat{x}}_2 &= -\Lambda_M^{-1}(\Lambda_C \hat{x}_2 + \Lambda_G) + \hat{d}(x,t) \\ &\quad + \Lambda_M^{-1} w_d + \zeta_2 sign(\tilde{x}_1) \end{aligned} \tag{7}$$

where $\hat{x}_i$ are the state estimations, $\tilde{x}_1 = x_1 - \hat{x}_1$, ζ_i are positive diagonal constant matrices, and $\hat{d}(x,t)$ is an estimate of $d(x,t)$.

Remark 3. Instead of the state observer presented in (7), the conventional high-gain state observer[1-4] can be written as

$$\begin{aligned} \dot{\hat{x}}_1 &= \hat{x}_2 + \zeta_1 \tilde{x}_1 \\ \dot{\hat{x}}_2 &= -\Lambda_M^{-1}(\Lambda_C \hat{x}_2 + \Lambda_G) + \hat{d}(x,t) + \Lambda_M^{-1} w_d \end{aligned} \tag{8}$$

3.2 Design of Backstepping Terminal Sliding Mode Controller

We define the tracking error as follows:

$$z_1 = \hat{x}_1 - y_d, \tag{9}$$

where y_d is the desired position or trajectory. The time derivative of (9) is given as

$$\dot{z}_1 = \hat{x}_2 - \zeta_1 |\tilde{x}_1|^{1/2} sign(\tilde{x}_1) - \dot{y}_d. \tag{10}$$

Defining an virtual error variable as $z_2 = \hat{x}_2 - \alpha_1$, its derivative is expressed as

$$\begin{aligned} \dot{z}_2 &= \dot{\hat{x}}_2 - \dot{\alpha}_1 \\ &= -\Lambda_M^{-1}(\Lambda_C \hat{x}_2 + \Lambda_G) + \hat{d} \\ &\quad + \Lambda_M^{-1} w_d + \zeta_2 sign(\tilde{x}_1) - \dot{\alpha}_1 \end{aligned} \tag{11}$$

Defining the first Lyapunov function as follows:

$$V_1 = \frac{1}{2} z_1^T z_1 \tag{12}$$

its time derivative is given as

$$\begin{aligned} \dot{V}_1 &= z_1^T (\hat{x}_2 - \zeta_1 |\tilde{x}_1|^{1/2} sign(\tilde{x}_1) - \dot{y}_d) \\ &= z_1^T (z_2 + \alpha_1 - \zeta_1 |\tilde{x}_1|^{1/2} sign(\tilde{x}_1) - \dot{y}_d) \end{aligned} \tag{13}$$

Selecting a virtual control α_1 as

$$\alpha_1 = -c_1 z_1 + \zeta_1 |\tilde{x}_1|^{1/2} sign(\tilde{x}_1) + \dot{y}_d. \tag{14}$$

Substituting (14) into (13), we have

$$\dot{V}_1 = -c_1 z_1^T z_1 + z_1^T z_2. \tag{15}$$

To provide sufficient flexibility and robustness to uncertainty, we consider the following terminal sliding mode surface as:

$$s = z_2 + k_1 z_1 + k_2 |z_1|^{\gamma} sign(z_1) \tag{16}$$

where $k_1 \in R^n$ and $k_2 \in R^n$ are diagonal constant matrices and $0 < \gamma < 1$ is a constant.

We select the following control and adaptive laws as follows:

$$\begin{aligned} w_d = \Lambda_M [& -k_3 s - (k_1 + k_2 \gamma |z_1|^{\gamma-1}) \dot{z}_1 \\ & + \Lambda_M^{-1}(\Lambda_C \hat{x}_2 + \Lambda_G) - \hat{d}(x,t) \\ & - \zeta_2 sign(\tilde{x}_1) + \dot{\alpha}_1 - k_4 \frac{s}{\|s\| + \kappa}] \end{aligned} \tag{17}$$

$$\dot{\hat{d}} = \eta_d \|s\|, \tag{18}$$

where k_3 and k_4 are a positive diagonal matrix, $\kappa > 0$ is a constant, and η_d and ε_d are adaptive gains. In (17), if $z_1 = 0$ and $\dot{x}_1 \neq 0$, singularity may appear. In this case, z_1 is replaced by a small value $z_1 \approx \varepsilon$.

Remark 4. If the state observer in (8) is used instead of the observer given in (7), the control equations given in (14) and (17) are changed as

$$\alpha_1 = -c_1 z_1 + \zeta_1 \tilde{x}_1 + \dot{y}_d, \tag{19}$$

$$\begin{aligned} w_d = \Lambda_M [&-k_3 s - (k_1 + k_2 \gamma |z_1|^{\gamma-1}) z_2 \\ &+ \Lambda_M^{-1}(\Lambda_C \hat{x}_2 + \Lambda_G) - \hat{d}(x,t) \\ &- \zeta_2 \tilde{x}_1 + \dot{\alpha}_1 - k_4 \frac{s}{\|s\| + \kappa}] \end{aligned} \quad . \tag{20}$$

4. Stability Analysis

Define the second Lyapunov function as follows:

$$V_2 = V_1 + \frac{1}{2} s^T s + \frac{1}{2\eta_d} \tilde{d}^T \tilde{d}, \tag{21}$$

in which $\tilde{d} = d - \hat{d}$. The time derivative of (21) can be expressed as

$$\begin{aligned} \dot{V}_2 &= \dot{V}_1 + s^T \dot{s} + \frac{1}{\eta_d} \tilde{d}^T \dot{\tilde{d}} \\ &= -c_1 z_1^T z_1 + z_1^T z_2 + s[\dot{z}_2 + (k_1 + k_2 \gamma |z_1|^{\gamma-1}) \dot{z}_1] \\ &= -c_1 z_1^T z_1 + z_1^T z_2 + s^T [(k_1 + k_2 \gamma |z_1|^{\gamma-1}) \dot{z}_1 \\ &\quad - \Lambda_M^{-1}(\Lambda_C \hat{x}_2 + \Lambda_G + \Lambda_f) + \Lambda_M^{-1} w_d + \hat{d} \\ &\quad + \zeta_2 sign(z_1) - \dot{\alpha}_1] - \frac{1}{\eta_d} \tilde{d}^T \dot{\hat{d}} \end{aligned} \tag{22}$$

Substituting (17) and (18) into (22), we have

$$\begin{aligned} \dot{V}_2 &= -c_1 z_1^T z_1 + z_1^T z_2 - k_3 s^T s \\ &\quad + s^T \tilde{d} - \frac{1}{\eta_d} \tilde{d}^T \dot{\hat{d}} - k_4 \frac{s^T s}{\|s\| + \kappa} \\ &\le -c_1 z_1^T z_1 + z_1^T z_2 - k'_{34}(k_1 z_1 + z_2 + k_2 |z_1|^{\gamma} sign(z_1))^T \\ &\quad \times (k_1 z_1 + z_2 + k_2 |z_1|^{\gamma} sign(z_1)) \\ &= -k'_{34} [z_1^T \; z_2^T \; (sig^{\gamma}(z_1))^T] \\ &\quad \times \begin{bmatrix} c_1 + k_1^2 & k_1 - \frac{1}{2} & k_1 k_2 \\ k_1 - \frac{1}{2} & 1 & k_2 \\ k_1 k_2 & k_2 & k_2^2 \end{bmatrix} \begin{bmatrix} z_1 \\ z_2 \\ sig^{\gamma}(z_1) \end{bmatrix} + \|\tilde{d}\| \left(\|s\| - \frac{1}{\eta_d} \dot{\hat{d}} \right) \\ &\le -k'_{34\min} Z^T P Z \end{aligned} \tag{23}$$

where $Z = [z_1 \; z_2 \; sig^{\gamma}(z_1)]^T$, $sig^{\gamma}(z_1) = |z_1|^{\gamma} sign(z_1)$, $k'_{34\min} = \lambda_{\min}(k_3) + \frac{\lambda_{\min}(k_4)}{\|s\| + \kappa}$, and $P = \begin{bmatrix} c_1 + k_1^2 & k_1 - \frac{1}{2} & k_1 k_2 \\ k_1 - \frac{1}{2} & 1 & k_2 \\ k_1 k_2 & k_2 & k_2^2 \end{bmatrix}$.

If sufficient condition $c_1 + k_1 > 1/4$, P is a positive semi-definite symmetric matrix and the condition $-Z^T P Z \le 0$ is obtained. From the Lyapunov stability theorem, it is concluded that the tracking error will converge to equilibrium point in fast time in spite of disturbance and absence of velocity sensor by virtue of global sliding mode surface and estimations of unmeasurable velocity information as well as disturbance.

Next, we will discuss the stability of the state observer. From (6) and (7), the error equation is given as

$$\begin{aligned} \dot{\tilde{x}}_1 &= \tilde{x}_2 - \zeta_1 |\tilde{x}_1|^{1/2} sign(\tilde{x}_1) \\ \dot{\tilde{x}}_2 &= f - \zeta_2 sign(\tilde{x}_1) \end{aligned} \tag{24}$$

where $f = -\Lambda_M^{-1} \Lambda_C \tilde{x}_2 + \dot{d}$. Suppose that the system states can be bounded with the assumptions 1, 2, and 3, the existence of the upper bound constant f^+ of f is ensured such that the inequality

$$|f| < f^+ \tag{25}$$

holds for any possible t, x_1, x_2 and $|\hat{x}_2| \le 2 \sup |x_2|$.

Theorem 1. If the observer parameters are selected according to the following inequalities:

$$\begin{aligned} \zeta_2 &> f^+ \\ \zeta_1 &> \sqrt{\frac{2}{\zeta_2 - f^+}} \frac{(\zeta_2 + f^+)(1+p)}{1-p} \end{aligned} \tag{26}$$

where p is a constant and $0 < p < 1$. Then, the state variables of the observer in (7) converge in finite time to the states of the system (6), i.e., $\hat{x}_i \to x_i$.

Proof. See the result in [5].

Remark 5. The observer-based normal backstepping controller is designed for comparison with the proposed controller. Defining the Lypunov function as

$$V_2 = V_1 + \frac{1}{2} z_2^T z_2 \tag{27}$$

we can design the following observer-based normal back-stepping controller:

$$w_d = \Lambda_M[-c_2 z_2 - z_1 + \Lambda_M^{-1}(\Lambda_C \hat{x}_2 + \Lambda_G) - \hat{d}(x,t) - \zeta_2 sign(z_1) + \dot{\alpha}_1] \quad (28)$$

Remark 6. An observer-based nominal sliding mode back-stepping controller can be design by setting $\gamma = 1$ in (17) as follows:

$$w_d = \Lambda_M[-k_3 s - k_1 z_1 + \Lambda_M^{-1}(\Lambda_C \hat{x}_2 + \Lambda_G) - \hat{d}(x,t) - \zeta_2 sign(z_1) + \dot{\alpha}_1 - k_4 \frac{s}{\|s\| + \kappa}] \quad (29)$$

Remark 7. The chattering free sliding mode control scheme [12] if a large chattering in the control input of (29) appears. However, chattering under a normal condition is small because the sigmoid function instead of the signum is used in (29).

5. Application Examples

Fig. 1 shows the structure of the 2-axis rectangular robot control system,

$$M(q)\ddot{q} + C(q,\dot{q})\dot{q} + F_f + F_d = D(u) \quad (30)$$

in which deadzone appears due to misalignment between the motor axis and the ball-screw. In the robot system, the gravity dynamics do not appear in (1) because the 2-axis robot lies on the horizontal plane. In this system, $M(q)$ contains the unknown moment of inertia of each axis, which contains the inertia of the servo motors. The total friction torques come from the ball-screws, linear motion guides, and servo motors are included in F_d. The controller is designed not to include any dynamics or identify any of the parameters of the robot system. The specifications of the ball-screw, servo motors, and sensor are presented in Table 1. Three controllers are designed to evaluate the proposed control scheme: the backstepping controller with state observer (BC-OB), the backstepping and sliding mode control with state observer (BSMC-OB), and the proposed backstepping and terminal sliding mode control with state observer (BTSMC-OB). The hardware specifications of the robot system are presented in Table 1. The control system and signal flow are described in Fig. 1. The designed controllers are implemented via Matlab RTI library using MF624 board with 1kHz sampling frequency.

Table 1 Specifications of the 2-axis rectangular robot

Component	Specification
Servo motor	HP-KP23
Servo amplifier	MR-J3-20B
Lead of ball-screw	10mm (X, Y axis)
Motor power	200W(X-axis), 100W(Y-axis)
Resolution of linear scale	262144p/rev (X, Y axis)

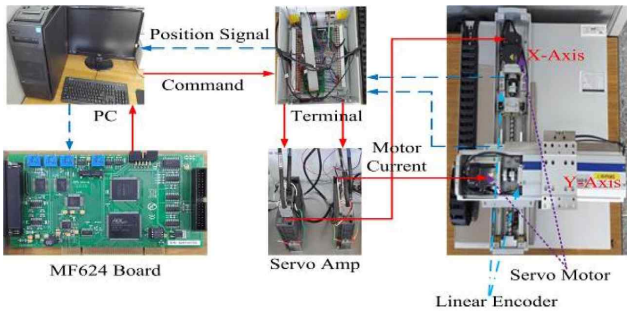

Fig. 1 Structure of the 2-axis rectangular robot system

5.1 Simulation Results

The control parameters were selected as $\Lambda_{Mx} = 0.005$, $\Lambda_{My} = 0.01$, $\Lambda_{Cx} = 0.001$, $\Lambda_{Cy} = 0.003$, $c_{x1} = 10$, $c_{y1} = 15$, $c_{x2} = 15$, $c_{y2} = 20$, $k_{x1} = 10$, $k_{y1} = 15$, $k_{x2} = 5$, $k_{y2} = 5$, $k_{x3} = 15$, $k_{y3} = 15$, $k_{x4} = 20$, $k_{y4} = 20$, $\zeta_{x1} = 10$, $\zeta_{y1} = 10$, $\zeta_{x2} = 5$, and $\zeta_{y1} = 5$. The command position signals were chosen as $y_{dx} = 5\sin(1.2566t)\,(mm)$ and $y_{dy} = 5\cos(1.2566t)$. Fig. 2(a) and (b) show the tracking output of two axes and the tracking errors in each axis are presented in Fig. 2(c) and (d), where it is shown that the error size of the proposed control system decreases greatly than those of other two systems.

The unmeasured states in each axis by the proposed observer in (7) are well estimated as shown in Fig. 2(e) and (f) comparing to the conventional observer in (8). Fig. 2(g) and (h) show the estimation errors. The estimated results for unknown disturbance are presented in Fig. 2(i) and (j). The control inputs of three control systems are shown in Fig. 2(k) and (l). Finally, the circle tracking results are shown in Fig. 2(m) and the circle tracking performance of the proposed BTSMC-OB system is superior than other systems. Therefore, these simulation results prove that the proposed control system has the improved performance than the conventional control systems. Simulation result for the vertical rectangular robot is presented in Fig. 3 to test the control performance on the gravity effect, where the proposed BTSMC-OB has also more improved control performance compared with other

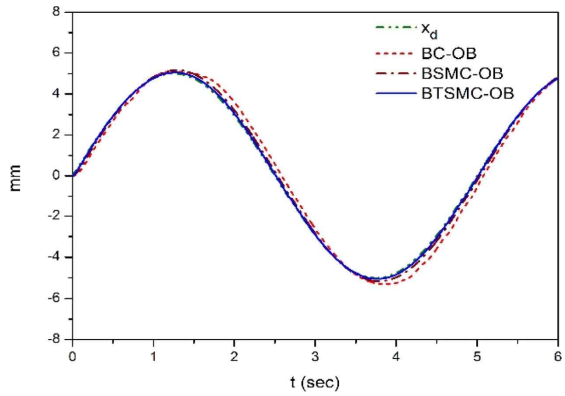

(a) Tracking output of x-axis.

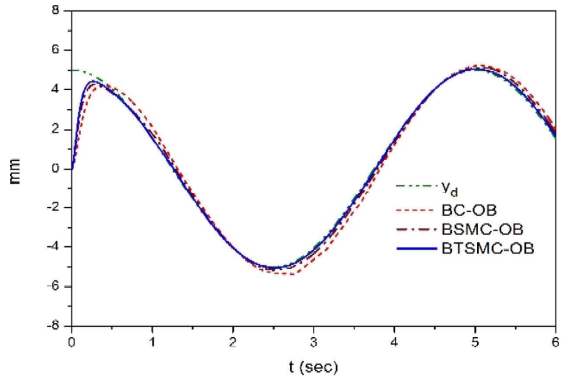

(b) Tracking output of y-axis.

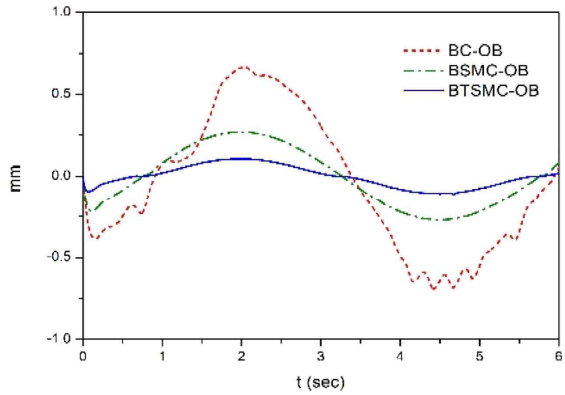

(c) Tracking error of x-axis.

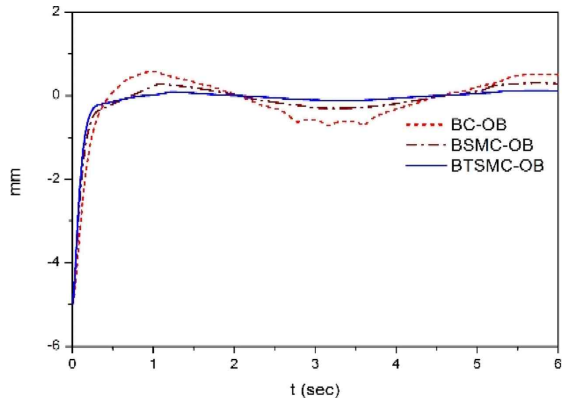

(d) Tracking error of y-axis.

Fig. 2 Simulation results for the horizontal rectangular robot

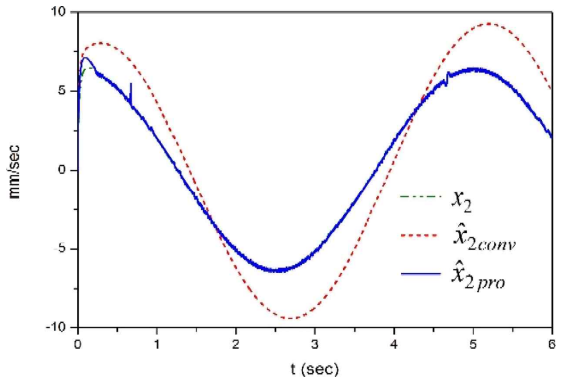

(e) Estimated results of the conventional observer and the proposed observer

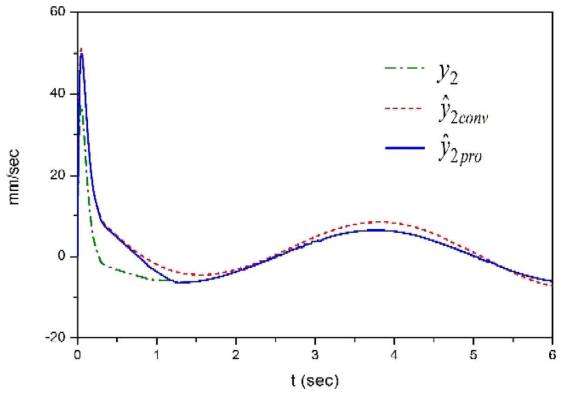

(f) Estimated results of the conventional observer and the proposed observer

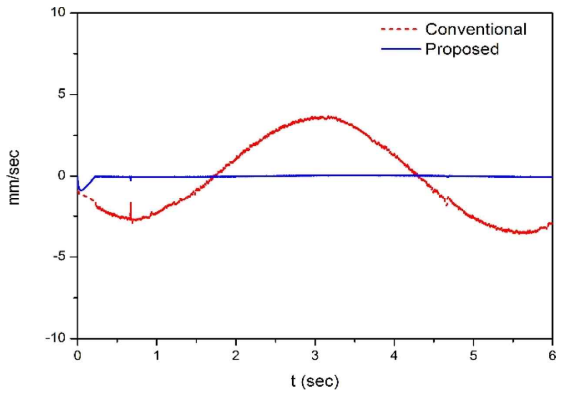

(g)

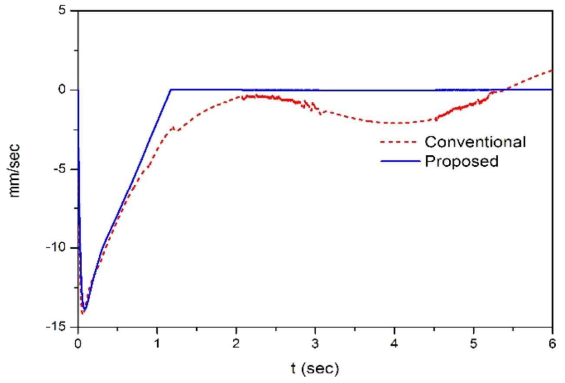

(h)

Fig. 2 Simulation results for the horizontal rectangular robot (continued)

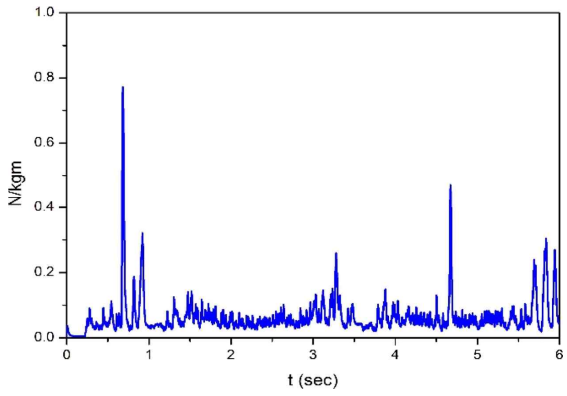

(i)

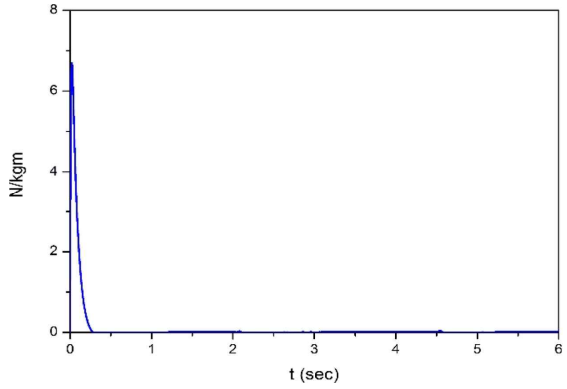

(j)

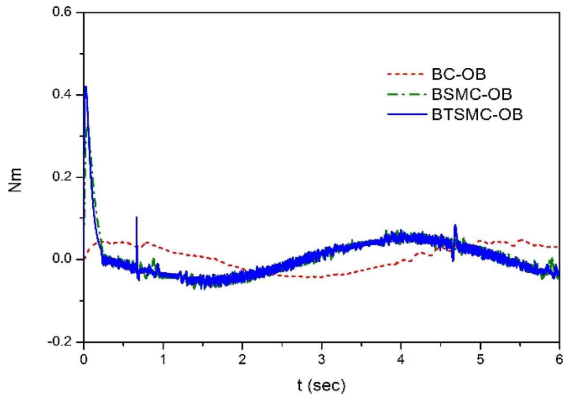

(k) Control input of x-axis.

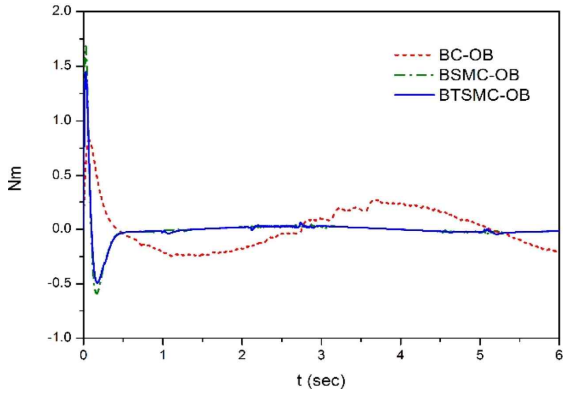

(l) Control input of y-axis.

Fig. 2 Simulation results for the horizontal rectangular robot (continued)

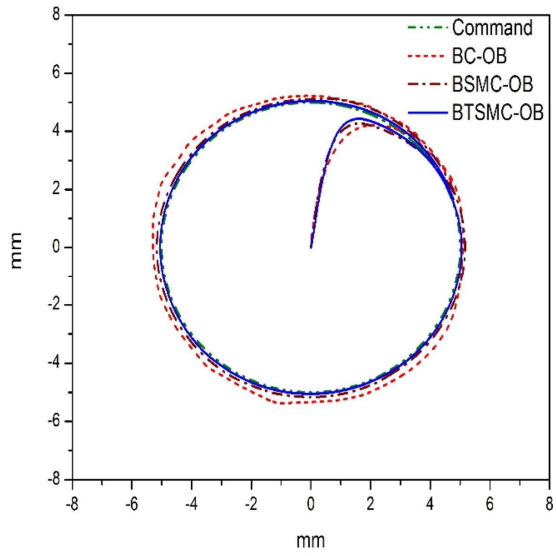

(m) Circle tracking output

Fig. 2 Simulation results for the horizontal rectangular robot (continued)

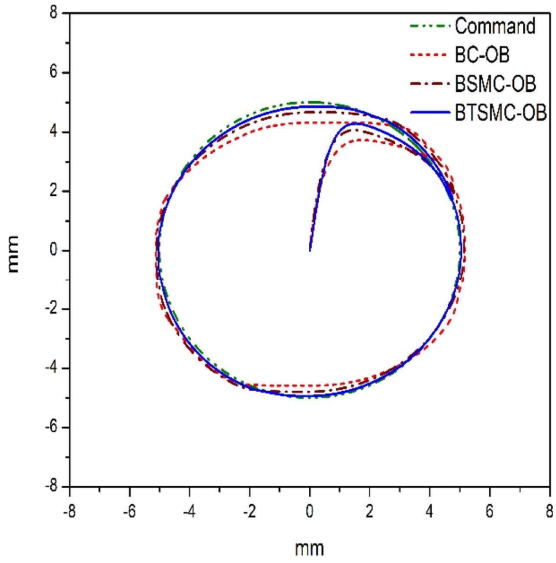

Fig. 3 Simulation result for the vertical rectangular robot

two systems. In the vertical robot where the y-axis is changed into the vertical z-axis and the x-axis remains in the horizontal axis, the gravity effect is reflected into increase of the vertical friction force because this system moves via ball-screw transformation device.

5.2 Experimental Results

The controller parameters in experiment were similarly selected like simulation case. The assumed deadzone widths were selected as $\hat{b}_{lx} = \hat{b}_{ly} = 0.025$ and $\hat{b}_{ly} = \hat{b}_{ly} = 0.1$. The command signals were selected like as simulation. For given

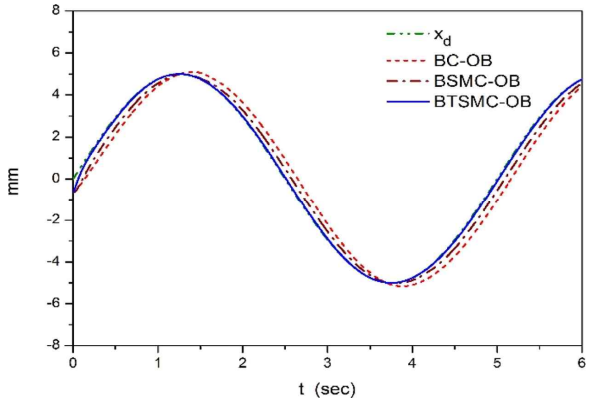

(a) Tracking output of x-axis.

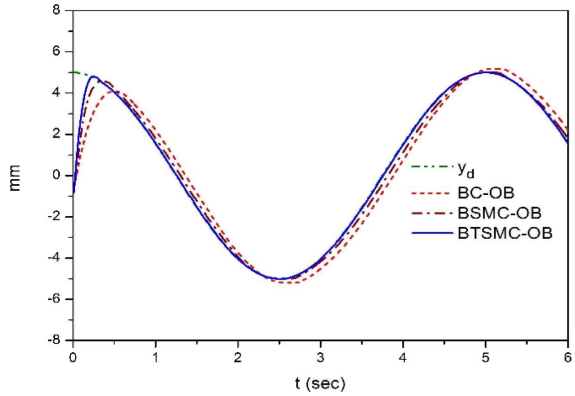

(b) Tracking output of y-axis.

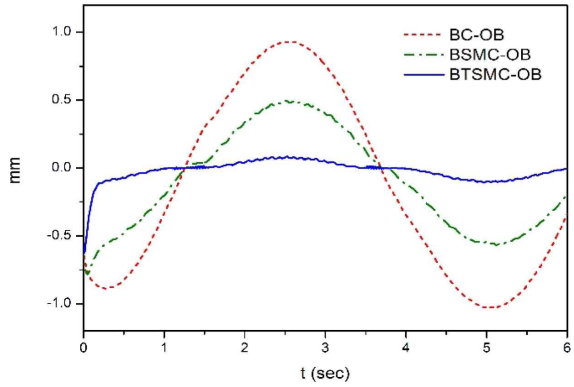

(c) Tracking error of x-axis.

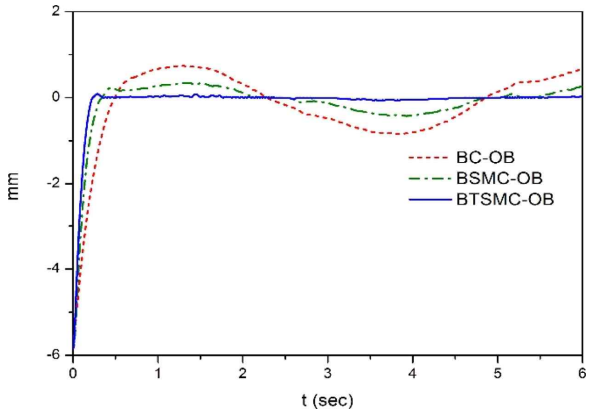

(d) Tracking error of y-axis.

Fig. 4 Experimental results

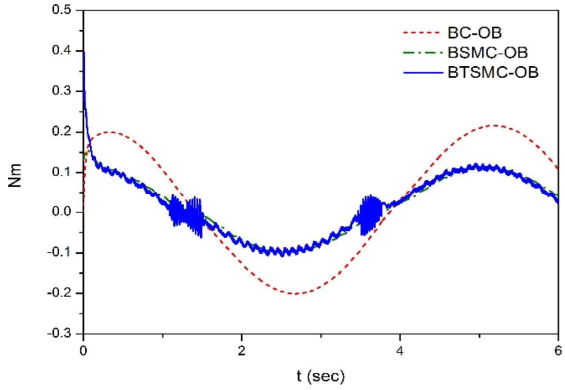

(e) Control input of x-axis.

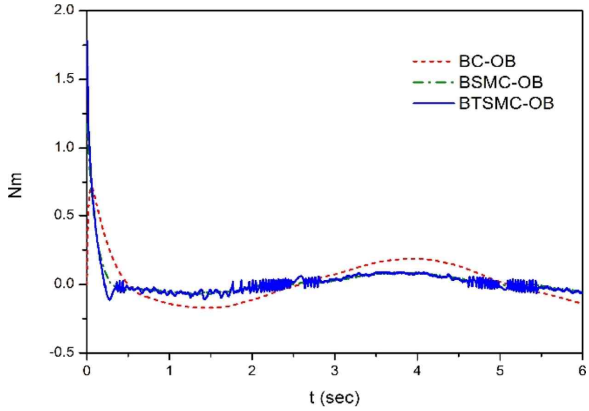

(f) Control input of y-axis.

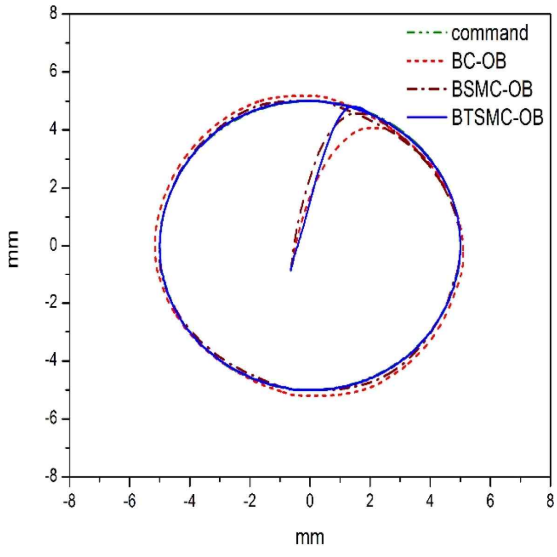

(g) Circle tracking output.

Fig. 4 Experimental results (continued)

circle command inputs, the tracking outputs in each axis are presented in Fig. 4(a) and (b). From these results, the tracking errors are shown in Fig 4(c) and (d), in which the tracking errors of the proposed system are very small than those of other two systems. The control inputs of three control systems are presented in Fig. 4(e) and (f). Finally, the circle tracking

outputs presented in Fig. 4(g) shows that the proposed control system has more superior performance than the conventional control systems.

6. Conclusions

In this paper, a super-twisting state observer and bactstepping control combined with terminal sliding mode surface is proposed to obtain conveniently the position controller in the reactangular robot system by introducing the pre-assumed dynamic parameters. The unmeasured states in the servo system can be more exactly estimated by using the super-twisting state observer. Backsteping control is considered to accommodate the state observer and the terminal sliding surface is introduced to enforce the robustness of the control system. Next, the unknown disturbance is estimated by designing adaptive law. The control performance of the proposed controller is tested via simulation and experiment for the 2-axis rectangular robot system. The results of simulation and experiment prove the efficacy of the proposed control system.

Acknowledgments

This work was supported by the National Research Foundation of Korea (NRF) Grant funded by the Korean Government (MSIP) (NRF-2015R1A2A2A01004457).

References

[1] Oh, S. G., Khalil, H. K., 1997, Nonlinear Output-Feedback Tracking Using High-gain Observer and Variable Structure Control, Automatica, 33:10 1845-1856.

[2] Lee, K. W., Khalil, H. K., 1997, Adaptive Output Feedback Control of Robot Manipulators, International J. of Control, 67:6 869-886.

[3] Atassi, A. N., Khalil, H. K., 2000, Separation Results for the Stabilization of Nonlinear Systems Using Different High-Gain Observer Designs, System & Control Letters, 39:3 183-191.

[4] Wang, C. H., Liu, H. L., Lin, T. C., 2002, Direct Adaptive Fuzzy-Neural Control With State Observer and Supervisory Controller for Unknown Nonlinear Dynamical Systems, IEEE Trans. Fuzzy Systems, 10:1 39-49.

[5] Davila, J., Fredman, L., Levant, A., 2005, Second-Order Sliding Mode Observer for Mechanical systems, IEEE Trans. A. C., 50:11 785-1789.

[6] Krstic, M., Kanellakopoulos, I., Kokotovic, P., 1995, Nonlinear and Adaptive Control Design, John-Wiley & Sons, New York.

[7] Tong, S. C., Li, Y. M., Shi, P., 2009, Fuzzy Adaptive Backstepping Robust Control for SISO Non-Linear System With Dynamic Uncertainties, Information Science, 179 1319-1332.

[8] Chen, M., Ge, S. S., How, B. V. E., 2010, Robust Adaptive Neural Network Control for a Class of Uncertain MIMO Nonlinear Systems With Input Nonlinearities, IEEE Trans. Neural Net., 21:5 796-812.

[9] Koshkouei, A. J., Zinober, A. S. I., Burnham, K. J., 2004, Adaptive Sliding Mode Backstepping Control of Nonlinear Systems With Unmatched Uncertainty, Asian J. of Control, 6:4 447-453.

[10] Yu, S., Yu, X., Shirinzadeh, B., Man, Z., 2005, Continuous Finite-Time Control for Robotic Manipulators With Terminal Sliding Mode, Automatica, 41 957-1964.

[11] Hu, C., Yao, B., Wang, Q., 2011, Adaptive Robust Precision Motion Control of Systems With Unknown Deadzones: A Case Study With Comparative Experiments, IEEE Trans. Indust. Electr., 58:6 2454-2464.

[12] Feng, Y., Han, F., Yu, X., 2014, Chattering Free Full-Order Sliding Mode Control, Automatica, 50, 1310-1314.

[13] Park, S. C., Lee, J. M., Han, S. I., 2018, Tracking Error Constrained Terminal Sliding Mode Control for Ball-Screw Driven Motion Systems with State Observer, Inter. J. Precision Eng. and Manufacturing, 19:3 359-366.